2. Model Photospheres and Chemical Compositions

https://doi.org/10.1017/S0252921100062734 Published online by Cambridge University Press

PHOTOSPHERIC MODELS FOR COOL GIANT STARS

M.S. Bessell[1] and M. Scholz[2]

[1] Mount Stromlo and Siding Spring Observatory
Canberra, Australia
[2] Institut für Theoretische Astrophysik
der Universität Heidelberg, Heidelberg, F.R.G.

Abstract. Models for M and C giant stars differ from those for hotter stars by having complicated state equations and opacities dominated by lines from diatomic and polyatomic molecules. In addition many cool giants have atmospheres which are extended, and which cannot therefore be adequately modelled using a plane-parallel approximation. Mira variable stars have atmospheres which are even more extended due to the regular passage of shock waves through their atmosphere. In this review we will discuss recent modelling of such atmospheres and show comparisons with observations of variable and non-variable M stars.

I. HISTORICAL OVERVIEW

Early attempts at constructing model atmospheres for cool stars were undertaken by Auman (1967,1969), Tsuji (1966), Alexander et al(1972), and Johnson (1974) for M stars (oxygen-rich, O/C >1), and by Querci et al (1974,1976), and Sneden et al (1976) for C stars (carbon-rich, O/C <1). Temperatures from models by Tsuji (1978) were shown to be in good agreement with the lunar occultation temperature scale for M stars (Ridgway et al, 1980), a significant success. Various methods of handling the complex line absorption opacities have been considered, mean opacities (eg Golden 1969; Tsuji 1966; Zeidler et al, 1982), Elsasser Band model (Tsuji 1968,1978), opacity distribution functions (ODF)(eg Querci et al 1971,1974; Gustaffson et al, 1975; Saxner et al, 1984) and opacity sampling (OS) method (eg Peytremann,1974; Sneden et al,1976). All this modelling was done under the assumption of plane-parallel (PP) geometry. More recent PP models for M stars have been published by Tsuji (1981), and Johnson et al (1980,OS). Steiman-Cameron et al (1986) compared these latter models with observations.

Schmid-Burgk et al (1975) surveyed the location of extended-photosphere stars in the HR diagram, and the properties of extended M-type photospheres were outlined by Watanabe et al (1978,1979); Schmid-Burgk et al (1981); Wehrse (1981), Scholz et al (1982), Kipper (1982) and Scholz (1985); and extended C-type photospheres by Scholz et al (1984). Scholz et al (1984) and Lambert et al (1986) found that extension was much less in C-type photospheres than in M-type photospheres of the same atmospheric parameters, but extension of C-type photospheres depended very sensitively upon the low-temperature opacities of carbon-rich element mixes, namely the hitherto little investigated polyatomic molecules such as HCN, C_2H and C_3 (Jørgensen et al 1985, 1987). Detailed discussions of extended model photospheres for M stars and comparison with observations have been given Scholz (1985), Brett (1988), and Bessell et al (1988a), hereinafter called BBSW1. Limb darkening and monochromatic radii of extended models (including miras) were discussed by Scholz et al (1987). Extension of atmospheres of pulsating stars caused by periodic shocks were investigated by Fedorova (1973), Wood (1979) and Bowen (1988). Exploratory extended atmospheres for mira-type variable M stars based on Wood's dynamical models were discussed by Bessell et al (1988b), hereinafter called BBSW2. More extensive analysis of model photospheres for miras of different period and composition, and at various phases, is underway.

In this review we will outline some of the complications associated with such modelling and show comparisons between recent model computations and observations.

https://doi.org/10.1017/S0252921100062734 Published online by Cambridge University Press

II. MODELLING PROBLEMS CONCERNING COOL PHOTOSPHERES

1. Obtaining opacities.

(a) Cool models involve complicated state equations with large number of composed particles (including dust at very low temperatures).
(b) Missing particles (in particular at very low temperatures) in the state equation may lead to spurious particle pressures of the absorbing particles.
(c) Poorly known physical input data of the state equation (cf. revisions of TiO and CN dissociation energy in the past) may lead to spurious partial pressures of the absorbing particles.
(d) Absorption is dominated by very large numbers of lines, in particular molecular-band lines (plus dust at very low temperatures). Missing absorbers (in particular at very low temperatures) may lead to grossly incorrect opacities.This is especially a problem for element mixes with C/O ≥ 1 or ≈ 1.
(e) Oscillator strengths of important bands may be unknown or poorly known (cf. several TiO bands, VO, HCN, C_3 etc).

2. Handling opacities.

(a) Continuum (H^-, H_2^-) is fading away towards low temperatures and opacities become line-dominated.
(b) Treatment of molecular lines by the mean-opacity technique reduces the required computer capacity (storage, time) but may be seriously inadequate, in particular for saturated lines.
(c) Treatment of lines by the ODF or the OS techniques requires large computer capacity. OS is more flexible, including the treatment of macroscopic velocity fields.
(d) Complicated molecules (e.g. H_2O, HCN, C_3) with complicated line patterns are hardly treatable with line-by-line techniques like ODF or OS.

3. Modelling and analyzing the photosphere.

(a) Strong wavelength dependence of opacities may lead to difficulties in finding the stratification which fulfills the energy equation, in particular via temperature correction methods which use weighted mean opacities (e.g. Lucy).
(b) Very accurate modelling is required if an important absorber which has great influence upon the stratification reacts sensitively to stratification changes (e.g. H_2O, HCN, C_3).
(c) Gravity sensitive features are hard to find at very low temperatures.
(d) Since all elements are coupled with each other via the composed particles in the state equation, a consistent set of element abundances has to be determined instead of carrying out an element by element analysis.
(e) Since absorption is dominated by lines, the abundance input for model construction and the abundances deduced from analysis have to be checked carefully for consistency. Not even the continuous absorption is a safe pre-given quantity because the free e^- forming H^- and H_2^- depend on the abundances of the alkali-earth and the alkali metals (which are less easily accessible than the Fe-type metals supplying the free e^- in hotter stars).
(f) An element or molecule which is not accessible by observation may still be important concerning (d) and (e).

III. MODELLING PROBLEMS CONCERNING GIANT PHOTOSPHERES

1. Modelling the photosphere.

(a) Non-variable (static) stars: Density or gas pressure scale height (scaled with the radius)

$$\frac{H_\rho(r)}{r} \approx \frac{H_{P_g}(r)}{r} = \frac{1}{r}\frac{\Re T}{\mu g_{eff}} \propto \frac{T_{eff}}{R g_s} \propto \frac{\sqrt{L}}{T_{eff} M}$$

is large for high-luminosity, low-mass giants (not as large for supergiants) meaning extended photospheres.

https://doi.org/10.1017/S0252921100062734 Published online by Cambridge University Press

(b) Mira (pulsating) stars: $H_\rho(r)/r$ is large because outgoing shock fronts produce flat density gradients between fronts; dynamical models imply more extended photospheres.
(c) Extension effects are important for extensions > 5%. (i) Dilution of radiative energy is proportional to $1/r^2$. Quasi plane modelling i.e. plane stratification with $1/r^2$ modification of radiative flux, is possible up to ??%. Needs to be tested. (ii) Peaking of radiation. Cannot be approximated in any modified PP approximation.
(d) Extension requires radius definition. Flat density gradient leads to noticeable photospheric mass fractions. Both reasons demand careful fitting of interior and photospheric models.
(e) Dynamical models should treat consistently the interior and photospheric layers.
(f) Grids of extended static model photospheres with given element mixture must be three-dimensional (L,M,R) or (T_{eff}, g_s, extension) rather than two-dimensional (T_{eff},g_s).
(g) Dynamical models should take into account the possibly slow relaxation of the heated post-shock material towards local thermodynamic dissociation and radiative equilibria.
(h) Dynamical models should take into account the radial macroscopic velocity fields modifying the line absorption coefficients used for model construction.
2. Analysing the photosphere.
(a) Because of low densities, deviations from LTE may be important (possibly also relevant for modelling).
(b) Because of possibly slow relaxation of the heated post-shock material of a dynamical model, deviations from LTE may be very strong (possibly also relevant for modelling).
(c) In the case of large extension, analysis of a static photosphere may yield three parameters (L,M,R) or (T_{eff}, g_s, extension) rather than only two (T_{eff}, g_s).
(d) Analysis of lines of a mira spectrum must take into account the radial macroscopic velocity fields affecting the line absorption coefficients.
Remark : up to some extension limit ??% (see 1c.), analysis of a line profile by means of a plane code is possible if the density-temperature-stratification of a quasi-plane ($1/r^2$) or extended model is used. (We intend to publish our T, Pg, r, rhox stratifications from an extended code and believe that they could be so used to good approximation.)
3. Monochromatic radii.
(a) Extended atmospheres have wavelength-dependent radii. Radius measurements must be carefully evaluated by using models for proper interpretation and for deriving a suitable $R(T_{eff})$ of the star.
(b) Monochromatic radii may be used as probes of the photospheric stratification.

IV. DETAILS OF EXTENDED MODEL CONSTRUCTION

The following discussion concerns mainly the spherical models of Scholz (1985) and BBSW1,2.
1. The static models are in radiative and hydrostatic equilibrium:

$$4\pi r^2 \pi F_{rad} = L$$

$$\frac{dP_g}{dr} = \frac{dP}{dr} + \rho k_F \cdot \frac{\pi F_{rad}}{c} = \rho \frac{GM}{r^2}\left(1 - k_F \frac{G}{4\pi c}\frac{L}{M}\right)$$

where r is the distance from the star's center, k_F is the flux-weighted mean opacity , other symbols have usual meaning. Convective energy transport does occur in red giant photospheres but is negligible. The radiative acceleration term is usually not important and turbulent acceleration is here neglected. The radiation transport equation is

$$\cos\theta \frac{\partial I_\nu}{\partial r} + \frac{\sin^2\theta}{r}\frac{\partial I_\nu}{\partial \cos\theta} = -\rho k_\nu (I_\nu - S_\nu)$$

https://doi.org/10.1017/S0252921100062734 Published online by Cambridge University Press

where θ is the polar angle in spherical coordinates, I_ν is the intensity in frequency ν and the source function S_ν is expressed in LTE by the Planck function B_ν and the mean intensity J_ν: $k_\nu S_\nu = \kappa_\nu B_\nu + \sigma_\nu J_\nu$. The monochromatic opacity k_ν is the sum of the LTE absorption and the scattering coefficients: $k_\nu = \kappa_\nu + \sigma_\nu$. The first equation of radiative equilibrium above is equivalent to the condition of vanishing radiative flux gradient,

$$\int_0^\infty k_\nu (J_\nu - S_\nu)\, d\nu = 0,$$

which is very sensitive to violations of the radiative equilibrium condition in the upper model layers.

The models discussed by BBSW1,2 were computed with a code based on the Schmid-Burgk method (Schmid-Burgk et al, 1984) of solving the spherical radiation transport equation. They were iterated for a flux constancy of 0.01% and radiative flux gradient of 1% (usually much better than these values). The LTE approximation is used to solve the equation of state and to calculate absorption and continuum scattering coefficients which are averaged over 72 wavelength meshes for model construction (Scholz et al 1984; Tsuji 1978). The absorption coefficients used were mean absorption coefficients, smeared over finite wavelength intervals.

The stellar radius R, which is the third basic photospheric parameter besides L and M, enters the system of equations through the outer boundary conditions: $P(r_0) = P_0$ and $I_\nu(r_0, \theta) = 0$ for $\theta < 0$, where r_0 denotes the transition layer from the photosphere to any other "non-photospheric" outer atmospheric region. This r_0 is a poorly defined quantity and in extended photospheres can be considerably larger than the observed radius or the outer boundary of an interior model. For many models it is adequate to define the radius R as the distance from the center of the star to the point where the standard optical depth (Rosseland mean opacity) is 1, and to define r_0 to be the distance to the point where the optical depth is 10^{-5}. See Scholz (1985) for details.The extension d is defined as:

$$d = (r_0 - R)/R .$$

(When $d \ll 1$, the atmosphere is called compact . For $d<0.05$ to 0.1 the atmosphere can often be treated in the plane-parallel approximation). The effective temperature T_{eff} can defined by the relation

$$T_{eff}^4 = L/[4\pi a R^2 (\tau_{Ros} = 1)].$$

There is an alternative definition of radius and efective temperature that is useful for interior models esp. with $T_{eff} < 3000$K. From the $T \sim r$ stratification of the model, if one evaluates the quantity $L/(4\pi a r^2)$ at each value of r and compares it with the quantity T^4(T is the temperature at r), then at some radius $r = \tilde{R}$, T will equal $(L/(4\pi a r^2))^{1/4}$. This temperature can be defined as the effective temperature T_{eff} and $\tilde{R}$ can be defined as the radius of the star. That is

$$T_{eff} \equiv T(\tilde{R}) = (L/(4\pi \tilde{R}^2))^{1/4}$$

In this definition, the stellar radius R does not depend on the special choice of reference τ scale, but it does depend sensitively on the photospheric temperature profile and on the model and opacity details. Some of our coolest models near 2200K produced differences of almost 200K from the two definitions, T_{eff} being less than Teff. These aspects are more fully discussed by BBSW2.

2. In the mira models that we have constructed, the condition of hydrostatic equilibrium is not imposed, instead, $\rho(r)$ or $P_g(r)$ is adopted from a dynamic envelope configuration. Wood (1979, 1989) computes non-adiabatic pulsating envelope-atmophere models using grey opacities. The configuration of exploratory models (BBSW2) were based on typical density profiles, at specific phases, of older pulsation models, with the density steps modified to agree with measured shock velocities (Hinkle et al, 1984). Recently we have started to use the actual structure from more realistic models, computed with specially computed Rosseland opacities for various metal mixes and temperatures between 10000K

and 750K. Scholz and Tsuji plan to compute similar carbon-rich opacities tables. The same technique as noted above is used to solve the spherical radiation transport and energy equations. LTE is assumed for the equation of state and opacity calculations.

3. Synthetic spectra computations.

The wavelength averaged opacity mesh used for model construction was too coarse to permit reasonable comparison with observed spectra, therefore an additional spectrum was computed for each model using a table of opacities at a much higher wavelength resolution. Several hundred wavelength points were computed down to 10Å resolution. Brett (1988) discussed the computation of these opacities and the comparison of the resultant spectra with observations of early M stars. Examples will be given below.

IV RESULTANT MODEL STRATIFICATIONS

1. Comparison with different techniques.

Scholz et al (1984) showed in the plane-parallel case, that the use of the smeared mean averaged opacities gave close to the same temperature stratification for models of early M stars as the OS technique of Johnson et al (1980). For the carbon-rich material the results were very different and they suspected that the carbon-rich line list used for the OS must be incomplete. Details of the Lambert et al (1986) carbon-rich model stratifications made using ODFs are not yet published, so a similar comparison cannot be made, however, Lambert et al note that IR fluxes from their models give a similar temperature calibration to that derived by Tsuji (1981) from his models based on the Elsasser Band model of mean opacities. These results support the proposition that mean-opacities can be used with cautious confidence for model building. The Elsasser Band model treatment is similar to construction of ODFs.

2. Comparison of different extended models.

Scholz (1985) found that usually (i) the temperature in the upper layers of the models decreases with increasing photospheric extension due to dilution of radiation and higher photon escape probability (in Fig.1a is shown the T(log P_g) stratification of three 3000K models with increasing photospheric extension): (ii) higher surface gravity shifts the T(P_g) curves towards higher pressures by $\Delta \log Pg \approx \Delta \log g_s$; and (iii) lower metal abundances shift the T(P_g) curves towards higher pressures due to the higher average transparency of matter. The main absorbers in O-rich atmospheres H^-, TiO, CO and H_2O react differently to abundance changes and are efficient at different temperatures in different layers, consequently the T(Pg) curves can have quite different shapes for models with different chemical compositions, different effective temperatures and different extensions. Water vapor plays an important role in this behaviour. When H_2O begins to form it acts as an efficient cooling mechanism, causing a steepened temperature gradient in these layers. Polyatomic molecules including C such as HCN and C_3 very likely produce the same effects in C stars.

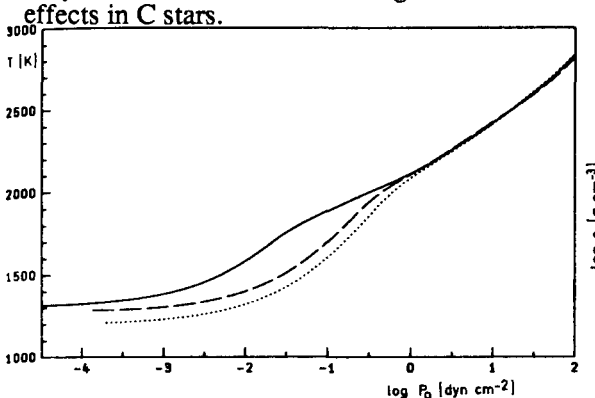

Figure 1a.

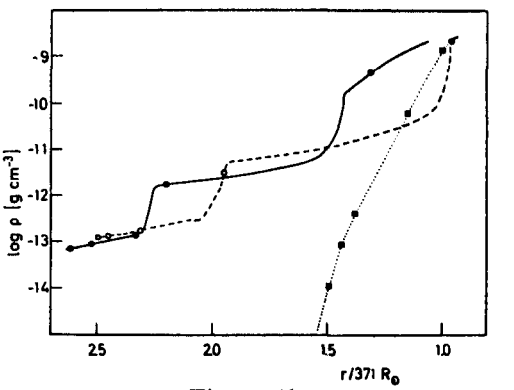

Figure 1b.

https://doi.org/10.1017/S0252921100062734 Published online by Cambridge University Press

In Fig.1b the T(r) stratification of two mira models is shown in comparison with a static model. The lowest temperature points marked on the curves indicate mean Rosseland optical depths of 10^{-4} so that one can see that the mira models have more than 3 times the extension of the static model which has d = 0.54. Scholz et al (1987) show that in such models the radius measured at the wavelength of a strong TiO band will be more than twice that measured in a continuum window. These model predictions agree nicely with the monochromatic radius observations for miras reported by Labeyrie et al (1977) and Bonneau et al (1982). Some of the models investigated were so extended that, owing to special conditions of density and opacity stratification, evidence of faint emission by H_2O was seen in the spectra. In such cases, slight limb-brightening is also possible (Scholz et al 1987).

The formation of H_2O is enhanced by low temperatures and high pressures, therefore H_2O opacity becomes important in high gravity models at a higher effective temperature than in a low gravity model, and is stronger in an extended model compared to a less extended model of the same T_{eff} and g. Scargle et al (1979) noted that the IR spectra of Tsuji's dwarf models resembled their observed mira spectra more than the giant and supergiant spectra. We can understand this now on the basis of the cool extended atmospheres of the mira models.

In the hotter models of M stars the extension d varied approximately linearly with the pressure scale height, however, in those models where H_2O formation became important, the extension doubled for little change in the pressure scale height, reflecting the increased opacity in the cool upper layers due to the polyatomic absorber. We anticipate that polyatomic absorbers will be similarly extremely important in extending the atmospheres of cool carbon-rich models.

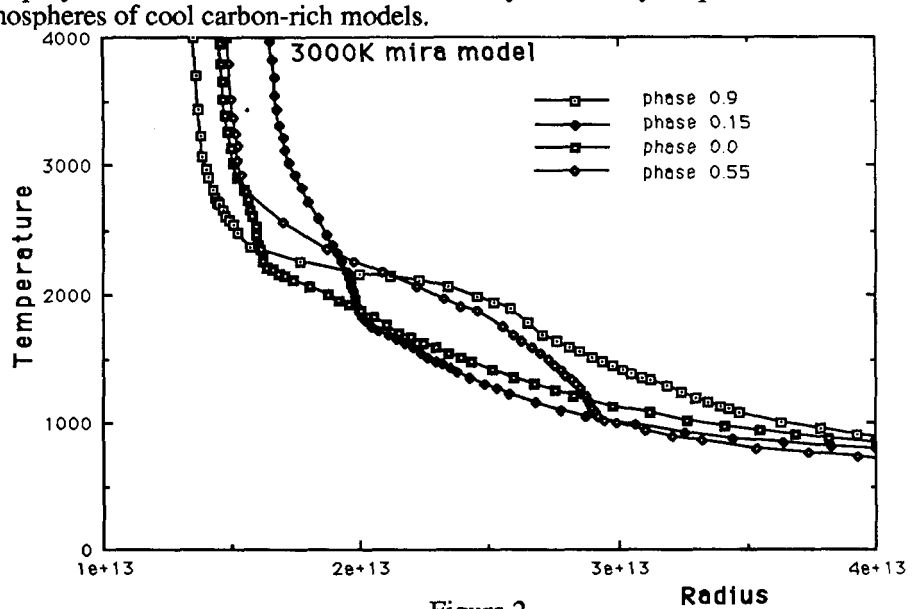

Figure 2.

In Fig.2 are shown the the T and r stratification at 4 phases, of some very preliminary self-consistent 3000K mira models. These show nicely the change in the temperature and density profiles as the shock-wave traverses the atmosphere. Wood's modelling assumes that the material behind the shock rapidly reaches radiative and thermodynamical equilibrium, whereas other workers, eg. Fedorova (1978) and Bowen (1987) use very approximate approaches for treating the de-excitation of the heated gas

https://doi.org/10.1017/S0252921100062734 Published online by Cambridge University Press

behind the shock-front. We show below that the Bowen (1988) T and ρ stratification results in unrealistic photospheric spectra compared to observations and that Wood's assumptions therefore are more likely to be correct.

V. RESULTANT PHOTOSPHERIC SPECTRA

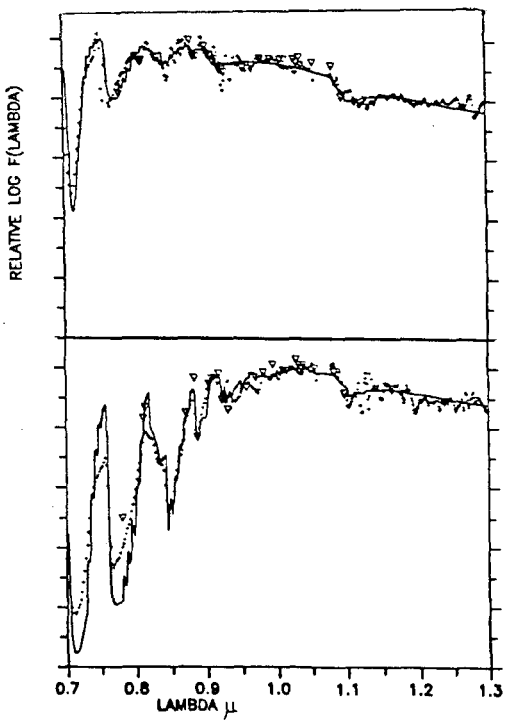

1. In Fig.3 are shown the near-IR spectra of some of our static models in comparison with observations. The top panel shows M3III observations and the 3650K model flux. The bottom panel shows M5III observations and the 3350K model flux.The observations are from Gunn and Stryker (1983) and Wing (1967). These comparisons are from Brett (1988). Spectral types were adopted from Wing (1978). The extension and gravity of the models were relevant for class III giants. The temperature scale thus indicated is in good agreement with the scale of Ridgway et al (1980), and the model spectral features are similar to observations. The grid of static spectra are discussed in detail in BBSW1.

Figure 3.

Fig.4 shows the calibration of two colors which have been used for temperature derivation in M stars. Both colors are reasonably insensitive to extension and gravity, as long as H_2O absorption is weak. Amongst the many features calculated, the TiO and H_2O bands were found to be most sensitive to the extension, while the CN and CO bands were very sensitive to the gravity, however, both effects must be accounted for in fitting data.

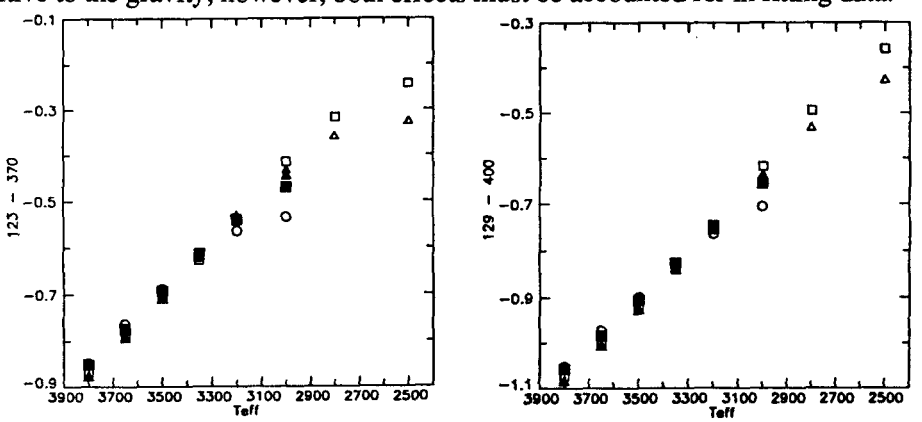

Figure 4.

https://doi.org/10.1017/S0252921100062734 Published online by Cambridge University Press

Fig.5 shows the variation of an IR color measuring the H_2O for giant models with different gravity and extension. The solid squares and open circles are higher gravity, low extension models; the open squares are more extended models than the open triangles, but have the same low gravity. Fig.6 shows the variation of a color measuring the CO second-overtone bands. The difference in gravity between the open square-triangle sequence and the open circle (higher gravity) sequence is 1.3 in log g. Details are given in BBSW1.

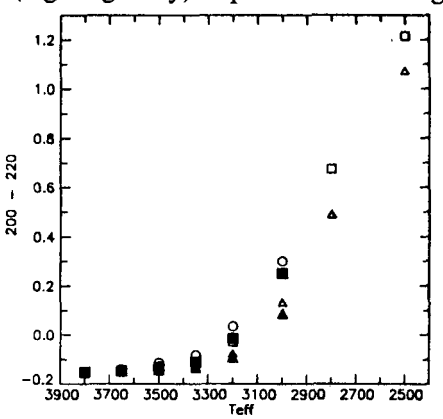

Figure 5.

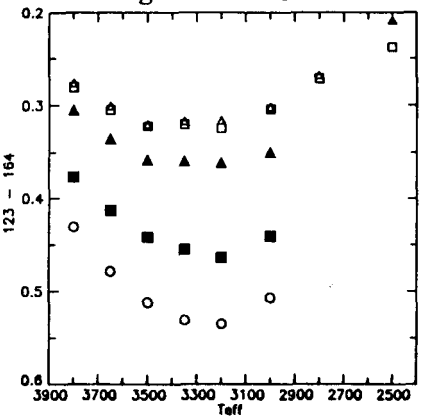

Figure 6.

In cool M stars, the IR broad-band magnitudes measure spectral regions which contain a variety of spectral features. In Fig.7 the photometric bands are shown with respect to the spectrum of a T_{eff} = 3000K, log g = -0.70, d = 0.54 model. Strong CO absorption is seen in the H and K bands, while H_2O is beginning to be seen in both wings of the H and K bands and the blue wing of the L band. In the J band TiO and VO are beginning to strengthen. The subsequent behaviour of the broad-band colors can be appreciated when one considers the modification of the continuum colors by the band absorption at cool temperatures.

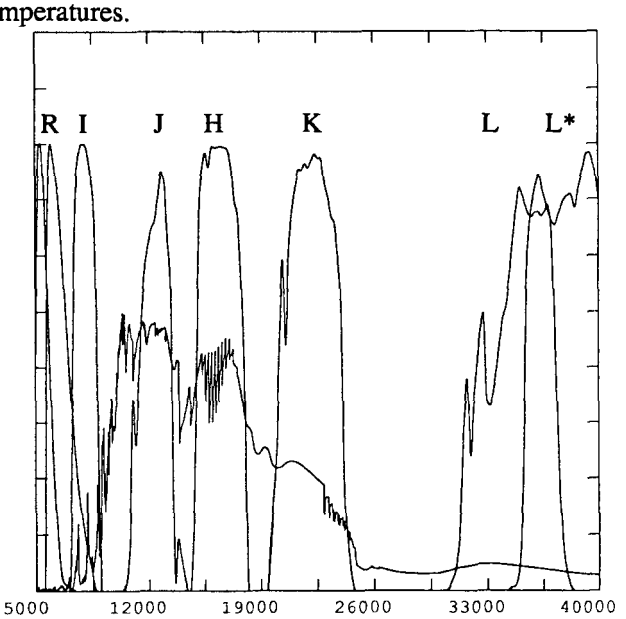

Figure 7.

https://doi.org/10.1017/S0252921100062734 Published online by Cambridge University Press

Brett (1988) has investigated the CN and Zr composition of peculiar redgiants in the Magellanic Clouds using modified mean opacities for bands. He demonstrated that such an approach is capable of determining abundances in very cool giants, providing specific observations are made. In the late-M and S stars, CN bands and ZrO bands are often masked by strong TiO bands. This requires that the 1.08μ CN and the 9300Å bands be used.The 1.08μ region is impossible to reach with a CCD detector but will be achievable for faint objects with the new IR arrays. Brett (1988) used data from Smith et al (1985) and Wing (1967) to fit the red ZrO band. He found that for T ≥ 3000K no significant bands of ZrO appear in models with unenhanced Zr abundance, irrespective of the C/O ratio, consistent with the column density results of Piccirillo (1980). He intends to extend this investigation to the cooler mira models in future as many ZrO strong objects have been found amongst long period miras in the Clouds.

With regard to the relevance of the coolest static models, we note that the spectra and IR colors of a $T_{eff} \approx 3000$K model corresponds to a spectral type of ~ M7III. BBSW2 showed that semi-regular M-type variables were observed to have such IR colors but that most mira variables in the solar-neighbourhood had redder, or more extreme colors. It is likely therefore that mira models will be more relevant for temperatures below 3000K.

2. In Fig.8 we show the near-IR CCD spectra of some late-type stars, mainly miras.

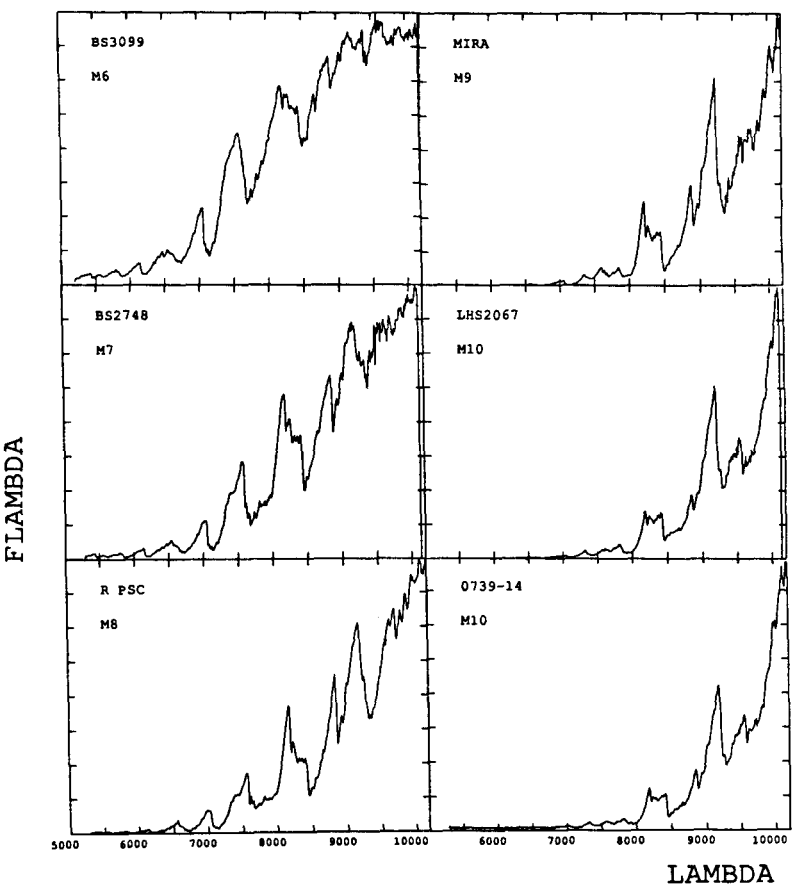

Figure 8.

https://doi.org/10.1017/S0252921100062734 Published online by Cambridge University Press

For comparison in Fig.9 are shown some model spectra. Although some of the strong bands are too strong in the models due to saturation not being taken into account in the mean opacities, the overall appearance of the model spectra, in particular the relative VO and TiO strengths, resembles that of the observations and indicates the relative effective temperatures corresponding to the later spectral types.

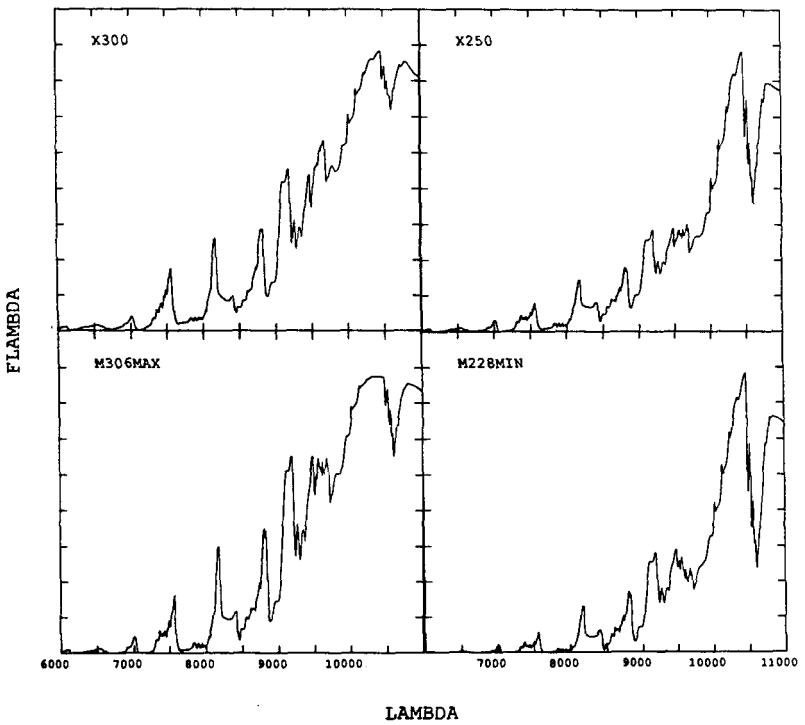

Figure 9.

BBSW2 investigated the spectral differences between static models and exploratory mira models with the same T_{eff}. They found that mira models had comparable continuum, or color temperatures to the static models but that the strength of the TiO γ 0,0 band near 0.7μ was similar to that of a static model 200K cooler. The redder TiO and VO bands also showed a difference, but not as large. As a result of this, different spectral types would be assigned to a mira model, depending on which TiO band was used. Such an observed effect had been long noted in mira variables (eg. Wing 1967). The phase of maximum (luminosity) mira models also have H_2O absorption similar to a static model 200K cooler, although the absorption in the minimum phase models were comparable to that in the static models. The greater strength of the H_2O absorption in the extended mira models results in the H, K and L fluxes, in particular H, being depressed.

One interesting aspect of the IR fluxes of both cool static and mira models is that black-body fitting to broad-band JHKL fluxes is not a sensitive way of determining effective temperatures. In Fig.10 are plotted the IR color temperature, so derived, and the model T_{eff}. It is clear that there is little change in the IR color temperature as T_{eff} changes from 3200K to 2500K. Also plotted are the data for some miras whose effective temperatures have been derived from lunar-occultation. In this aspect at least, the behaviour of the models clearly resemble that of real stars.

https://doi.org/10.1017/S0252921100062734 Published online by Cambridge University Press

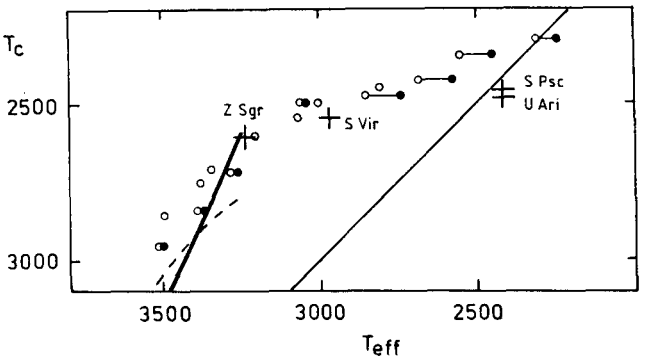

Figure 10.

In Fig.11 and 12 the IR spectra of two miras (one near maximum the other near minimum) with periods near 1 year are shown in comparison with the exploratory 3000K mira spectra of BBSW2. Although the H_2O bands in the models are deeper than in the stars, possibly another instance of saturation not being properly considered, the IR model spectra again showed encouraging similarity to the observations. Black-body fits to the integrated fluxes are also shown for instruction.

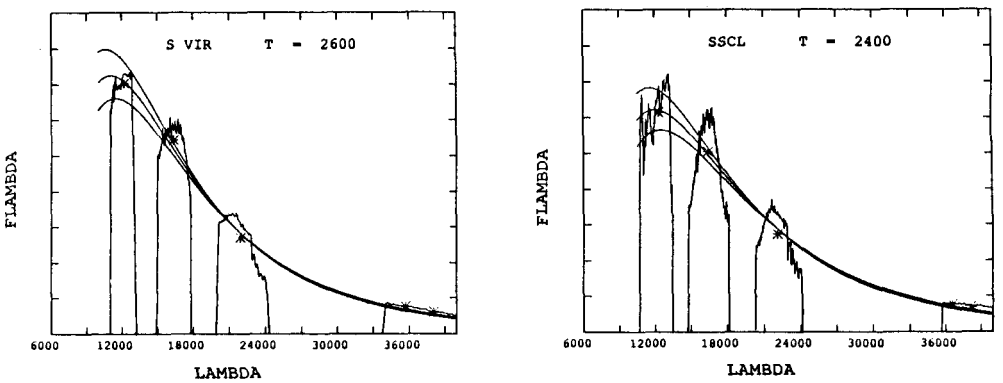

Figure 11.

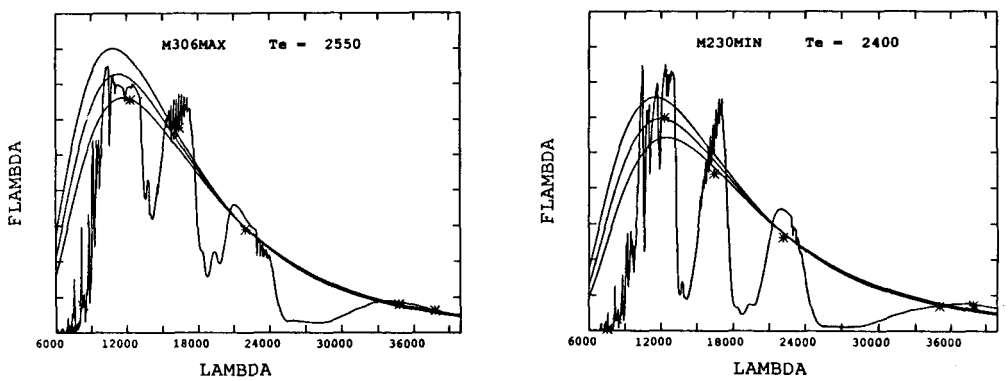

Figure 12.

https://doi.org/10.1017/S0252921100062734 Published online by Cambridge University Press

Very recently, Wood (1988) calculated a more realistic model for a $1.5M_{\odot}$, 300 day, 3000K mira pulsating in the fundamental mode. Several hundred models are computed for each pulsation cycle, and after a periodic behaviour was well established with a bolometric amplitude of 0.6mags, we selected models at particular phases in order to produce non-grey spherically symmetric model atmospheres based on the P_g, r stratification of the dynamical grey-models. In a preliminary examination for this conference we have computed 4 models at phases 0.9, 0.0, 0.15 and 0.55. The T and ρ stratifications were shown in Fig.2.

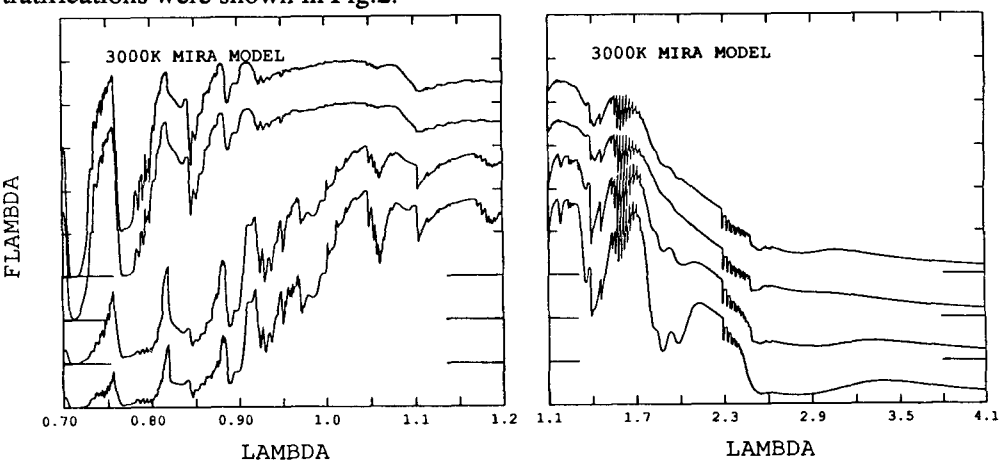

Figure 13.

In Fig.13 is shown the near-IR and the IR spectra of these models. The zero levels of each spectrum is offset as indicated on the ordinate. The T_{eff} for these models were about 3390K, 3330K, 2970K and 2850K respectively, and the general appearance of the near-IR spectra suggests that the spectral-type varies from M4-5 to M8, similar to observed for 300 day miras. The great strength of the TiO γ 0,0 band in the models near maximum luminosity is very spectacular and resembles that shown in published spectra of some Magellanic Cloud miras (Bessell 1983). Although such self-consistent modelling is in the earliest stages we are encouraged by the preliminary spectra and plan to investigate a range of periods, masses, luminosities and compositions.

An alternative approach to the modelling of mira atmospheres by Bowen (1988) and Beach et al (1988) was mentioned above. We have taken their published T and ρ stratification based on non-equilibrium assumptions, and computed a spectrum using ion and molecular abundances calculated from the LTE equation of state and the LTE absorption and scattering coefficients. This is of course, an inconsistent treatment but it should still give some clue whether or not this stratification is suited for interpreting the observed spectra of mira variables. In Fig.14 is shown the resultant spectrum.

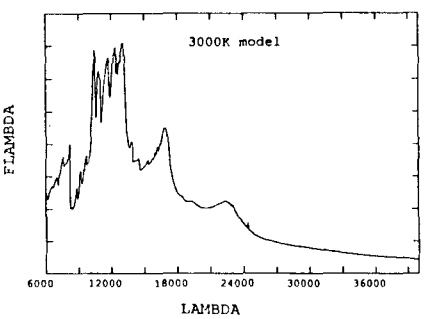

Figure 14.

https://doi.org/10.1017/S0252921100062734 Published online by Cambridge University Press

This is to be compared to the observed spectra of Figs.8, 11 and 12, and the model spectra of Fig. 13. Clearly, the spectra bear little resemblence to observations and we believe that this is good evidence that the Bowen stratification and hence their present approximations concerning rates of cooling behind the shock front are less realistic than the assumption of radiative equilibrium used by Wood. We note that our models completely neglect the hot region in the vicinity of the shock front which produces the hydrogen emission lines and UV MgII emission lines seen at some phases in mira variables, but we suggest that the region of excited material is confined to such a small volume that its effect on the bulk of the photospheric material is negligible at most phases.

VI. SUMMARY

The current modelling of the photospheres of M stars including mira variables is producing good agreement with many of the observed properties of such stars. Some of this work uses mean opacities which does not handle saturated bands so well as other techniques; however, adoption of Tsuji's use of the Elsasser Band model, which is equivalent to the ODF technique, will provide improvement. It would be of great interest to use the OS technique, together with the velocity gradient information, to produce more realistic spectra from our stratifications. Generally, the modelling of M stars has produced good insight into the interpretation of observations and we anticipate a very productive phase of M-S star analyses to follow.

Lambert et al (1986) discuss their grid of C-rich models and use the models to interpret high resolution spectra of C stars. These models appear to be excellent, but the authors comment on a few molecular features that do not fit the observations as well as they would like. They have not yet published the models or the fluxes or colors. Jørgensen et al (1988) is continuing the investigation of additional polyatomic molecules relevant for C stars. We intend to construct extended static and mira models for C stars using Tsuji's opacities, but Tsuji continually reminds us of the uncertainties associated with the polyatomic carbon molecules so important at cool temperatures. Nevertheless, we anticipate advances in the interpretation of C-rich stars also, following the publication of the Lambert et al model grid and of the Scholz-Tsuji study.

VII. REFERENCES

Alexander, D.R., Johnson, H.R. 1972, **Astrophys.J.** 176, 629
Auman, J.R. 1967, **Astrophys.J.Suppl.** 14, 171
Auman, J.R. 1969, **Astrophys.J.** 157, 799
Beach, T.E., Willson, L.A.,Bowen, G.H. 1988, **Astrophys.J.** 329, 241
Bessell, M.S. 1983, in **IAU Symposium No.108**, ed.Van Den Bergh, S., De Boer, K.p171
Bessell, M.S., Brett, J.M., Scholz, M., Wood, P.R. 1988a, **Astron.Astrophys.** in press
Bessell, M.S., Brett, J.M., Scholz, M., Wood, P.R. 1988b, **Astron.Astrophys.** in press
Bonneau, D., Foy, R., Blazit, A., Labeyrie, A. 1982, **Astron.Astrophys.** 106, 235
Bowen, G.H. 1988, **Astrophys.J.** 329, 299
Brett, J.M. 1988 **Astron.Astrophys.** submitted
Brett, J.M. 1988 Thesis ANU
Fedorova, O.V.1973, **Astrofizika** 14, 239
Golden, S.A. 1969, **Journal Quantit.Spectrosc.Radiat.Transfer** 9, 1067
Gunn, J.E., Stryker, L.L. 1983, **Astrophys.J.Suppl.** 52, 121
Gustafsson, B., Bell, R.A., Eriksson, K., Nordlund, A. 1975, **Astron.Astrophys.** 42, 407
Johnson, H.R. 1974, NCAR-TN/STR-95
Johnson, H.R., Bernat, A.P., Krupp, B.M. 1980, **Astrophys.J.Suppl.** 42, 581
Jørgensen, U.G., Almhof, J., Gustafsson, B., Larsson, M., Siegbahn, P. 1985, **J.Chem.Phys.** 83, 3034
Jørgensen, U.G., Almhof, J., Siegbahn, P. 1988, **J.Chem.Phys.** submitted
Kipper, T. 1982, W.Struve nimeline Tartu Astrofüsika Observatoorium 66, 3

Labeyrie, A., Koechlin, L., Bonneau, D., Blazit, A., Foy, R. 1977, **Astrophys.J.** 218, L75
Lambert, D.L., Gustafsson, B., Eriksson, K., Hinkle, K.H. 1986
Astrophys.J.Suppl. 62, 581
Petreymann, E. 1974, **Astron.Astrophys.** 33, 203
Piccirillo, J. 1980, **Mon.Not.Roy.astr.Soc.** 190, 441
Querci, F., Querci, M., Kunde, V.G. 1971, **Astron.Astrophys.** 15, 256
Querci, F., Querci, M., Tsuji, T. 1974, **Astron.Astrophys.** 31, 265
Querci, F., Querci, M.1976, **Astron.Astrophys.**49, 443
Ridgway, S.T., Joyce, R.R., White, N.M., Wing, R.F. 1980, **Astrophys.J.** 235, 126
Saxner, M., Gustafsson, B. 1984, **Astron.Astrophys.** 140, 334
Scargle, J.D., Strecker, D.W. 1979, **Astrophys.J.** 228, 838
Scholz, M. 1985, **Astron.Astrophys.** 145, 251
Scholz, M., Takeda, Y. 1987, **Astron.Astrophys.** 186, 200
Scholz, M., Tsuji, T. 1984, **Astron.Astrophys.** 130, 11
Scholz, M., Wehrse, R. 1982, **Mon.Not.Roy.astr.Soc.** 200, 41
Schmidt-Burgk, J., Scholz, M. 1975, **Astron.Astrophys.** 41, 41
Schmidt-Burgk, J., Scholz, M., Wehrse, R. 1981, **Mon.Not.Roy.astr.Soc.** 194, 383
Smith, V.V., Lambert, D.L. 1985, **Astrophys.J.** 294, 326
Sneden, C., Johnson, H.R., Krupp, B.M. 1976, **Astrophys.J.** 204, 281
Steiman-Cameron, T.Y., Johnson, H.R. 1986, **Astrophys.J.** 301, 868
Tsuji, T. 1966, **Pub.Astr.Soc.Japan** 18, 127
Tsuji, T. 1968, in **Low Luminosity Stars**, ed. S.Kumar, Gordon and Breach, N.Y., p.457
Tsuji, T. 1978, **Astron.Astrophys.** 62, 29
Tsuji, T. 1981, **J. Astrophys.Astron.** 2, 95
Watanabe, T., Kodaira, K. 1978, **Pub.Astr.Soc.Japan** 30, 21
Watanabe, T., Kodaira, K. 1979, **Pub.Astr.Soc.Japan** 31, 61
Wehrse, R. 1981, **Mon.Not.Roy.astr.Soc.** 195, 553
Wing, R.F. 1967, Thesis University of California, Berkeley
Wood, P.R. 1979, **Astrophys.J.** 227, 220
Wood, P.R. 1988, work in progress
Zeidler-K.T., E.-M., Koester, D. 1982, **Astron.Astrophys.** 113, 173